Morphology-dependent resonances of nearly spherical particles in random orientation

Michael I. Mishchenko and Andrew A. Lacis

We use precise T-matrix calculations for prolate and oblate spheroids, Chebyshev particles, and spheres cut by a plane to study the evolution of Lorenz–Mie morphology-dependent resonances (MDRs) with increasing asphericity of nearly spherical particles in random orientation. We show that, in the case of spheroids and Chebyshev particles, the deformation of a sphere by as little as one hundredth of a wavelength essentially annihilates supernarrow MDRs, whereas significantly larger asphericities are needed to suppress broader resonance features. The MDR position and profile are also affected when the deviation of the particle shape is increased from that of a perfect sphere. In the case of a sphere cut by a plane, the supernarrow MDRs are much more resistant to an increase in asphericity and do not change their position and profile. These findings are consistent with the widely accepted physical interpretation of the Lorenz–Mie MDRs.

OCIS codes: 290.0290, 290.2200, 290.4020, 290.5850.

1. Introduction

It is well known from the Lorenz–Mie theory that perfect dielectric spheres exhibit morphology-dependent resonances (MDRs) at natural frequencies of oscillation in the form of a high-frequency ripple structure and supernarrow spikelike features in the plots of various scattering characteristics versus size parameter $x = 2\pi a/\lambda$, where a is the sphere radius and λ is the wavelength in the surrounding medium.[1–3] Although the experimental demonstration of the Lorenz–Mie ripple structure presents little technical challenges, measuring the profiles of supernarrow MDRs (SNMDRs) can be a much more laborious task. However, there have been quite a number of successful laboratory measurements of the Lorenz–Mie SNMDRs,[3] which poses an interesting question of how much a real particle can deviate from an ideal sphere while still exhibiting a Lorenz–Mie SNMDR. Because nearly spherical particles are unlikely to have a preferential orientation during the time necessary to take a measurement in a typical experimental setting, answering this question requires precise numerical computations for nonspherical particles in random orientation. We address this problem by using the highly accurate and efficient approach[4] based on Waterman's T-matrix method.[5] The main advantage of this approach is that all orientation-averaged scattering characteristics are calculated analytically so that the computational accuracy and efficiency are not compromised by a quadrature scheme for the evaluation of integrals over the angles specifying the particle orientation with respect to the laboratory reference frame.

2. Spheroids and Chebyshev Particles

Figures 1–4 summarize the results of the T-matrix computations for spheres and randomly oriented nearly spherical spheroids and Chebyshev particles with a relative refractive index of 1.4 in the range of size parameters affected by the $a_{38}{}^1$ Lorenz–Mie resonance.[6] We follow the notation introduced in Ref. 7, which implies that $a_{38}{}^1$ is the first resonance generated by the a_{38} Lorenz–Mie coefficient as x increases from zero. The shape of the spheroids is characterized by the axis ratio a/b, where b is the spheroid semiaxis along the axis of rotation and a is the semiaxis in the perpendicular direction. The shape of a Chebyshev particle with respect to the particle reference frame is given by $r(\theta) = r_0[1 + \xi T_n(\cos\theta)]$, where r_0 is the radius of the unperturbed sphere, ξ is the deformation parameter, $T_n(\cos\theta) = \cos n\theta$ is the Chebyshev polynomial of degree n, and θ is the polar angle. Following Ref. 8, we denote

M. I. Mishchenko (mmishchenko@giss.nasa.gov) and A. A. Lacis (alacis@giss.nasa.gov) are with the NASA Goddard Institute for Space Studies, 2880 Broadway, New York, New York 10025-7848.

Received 10 April 2003; revised manuscript received 14 July 2003.

0003-6935/03/275551-06$15.00/0

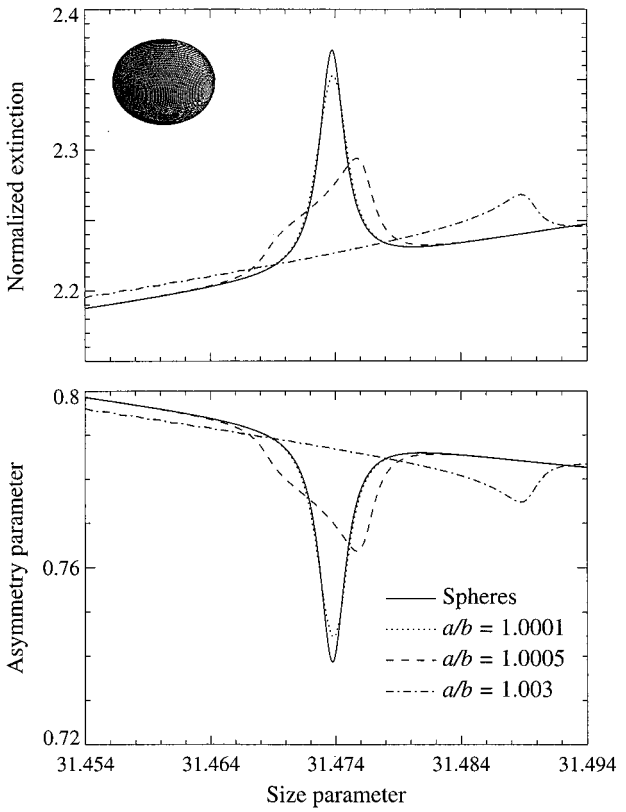

Fig. 1. T-matrix computations of the normalized extinction and asymmetry parameter for spheres and equal-volume oblate spheroids in random orientation in the neighborhood of the $a_{38}{}^{1}$ Lorenz–Mie resonance.

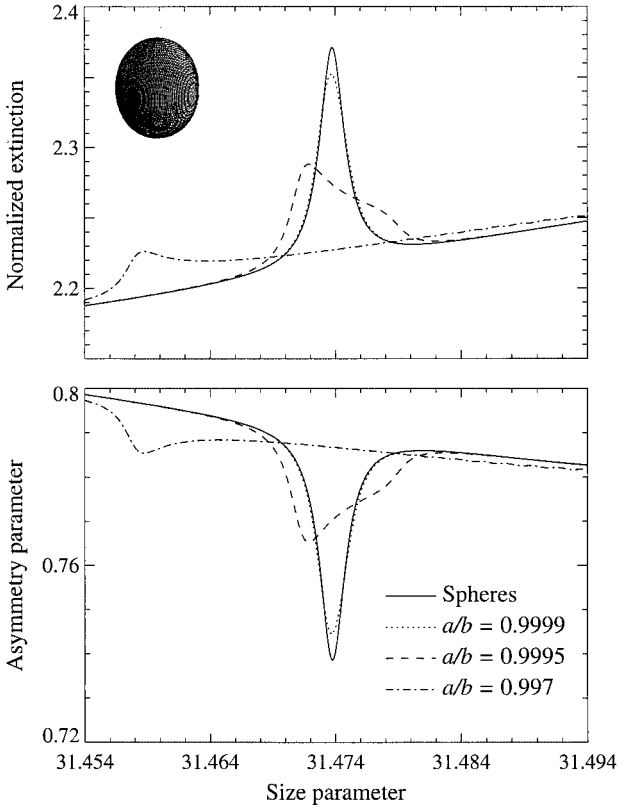

Fig. 2. As in Fig. 1, but for prolate spheroids.

Chebyshev particles by the notation $T_n(\xi)$. The size of the spheroids and Chebyshev particles relative to the wavelength is specified by the size parameter of the equal-volume sphere. The normalized extinction is defined as the ratio $\langle C_{\text{ext}}\rangle/(\pi a^2)$, where $\langle C_{\text{ext}}\rangle$ is the orientation-averaged extinction cross section and a is the radius of the equal-volume sphere. The asymmetry parameter is defined by Eq. (4.41) of Ref. 2. The relative accuracy of the T-matrix computations was set to be better than 10^{-10}. Furthermore, we ensured the accuracy of our numbers by using the extended-precision version of the T-matrix code.[2] To precisely depict the profile of the SNMDR, the T-matrix results were computed with a small size parameter step size of $\Delta x = 0.0003$. The inserts in Figs. 1–4 show the respective particle shapes, although the degree of particle asphericity is grossly exaggerated for demonstration purposes.

Prolate and oblate spheroids are well suited to model a simple deformation of the spherical shape caused by the stretching or flattening of the sphere as a whole, whereas the Chebyshev particles are a good model to simulate a small-amplitude high-frequency ripple (microscopic roughness) on the sphere surface. It can be seen that both types of deformation have the same overall effect on the Lorenz–Mie SNMDR. Specifically, increasing the aspect ratio of the spheroids (the ratio of the largest to the smallest spheroid semiaxis) and the absolute value of the deformation parameter ξ of the Chebyshev particles rapidly reduces the height of the normalized extinction peak and the depth of the asymmetry parameter valley. It is in fact remarkable that the deformation of a sphere by as little as one hundredth of a wavelength essentially annihilates the resonance. Secondary effects of an increase in asphericity are the shift of the resonance to either smaller or larger size parameters and the increase of the complexity of resonance structure, which makes the resonance look like a superposition of the main and one or more minor resonances. The latter observation is especially true of the Chebyshev particles. Interestingly, the direction in which the resonance is shifted with increasing asphericity is opposite for oblate and prolate spheroids and for Chebyshev particles with positive and negative deformation parameters. In fact, the spheroid curves in Figs. 1 and 2 corresponding to the same aspect ratios and the Chebyshev particle curves in Figs. 3 and 4 corresponding to the same $|\xi|$ look almost like mirror images of each other.

Figure 5 parallels Fig. 2, but shows the results for a much wider range of size parameters and captures three SNMDRs as well as broader resonance features. It is obvious that it takes significantly larger asphericities to suppress the broader MDRs.

An interesting feature of the curve for $a/b = 0.9$ in Fig. 5 is the minute high-frequency ripple superposed on a slowly and weakly varying background. This

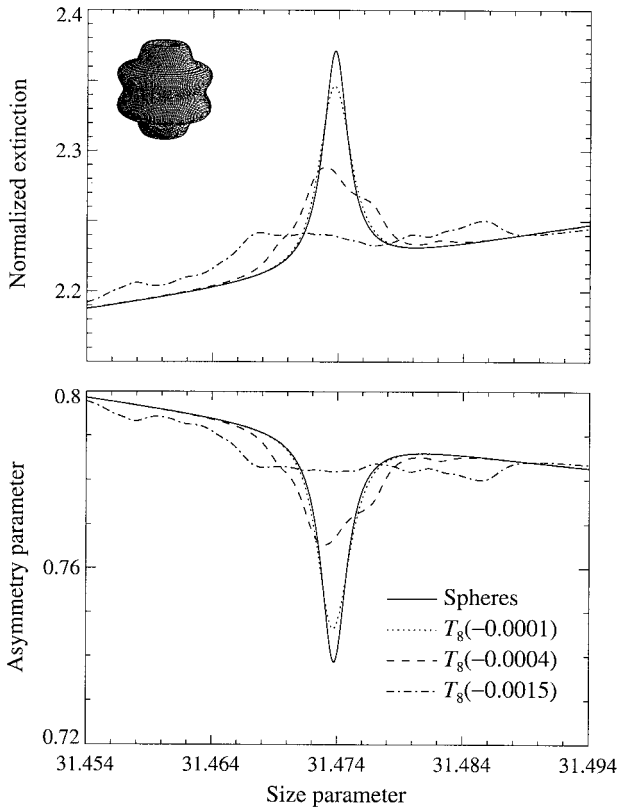

Fig. 3. As in Fig. 1, but for Chebyshev particles.

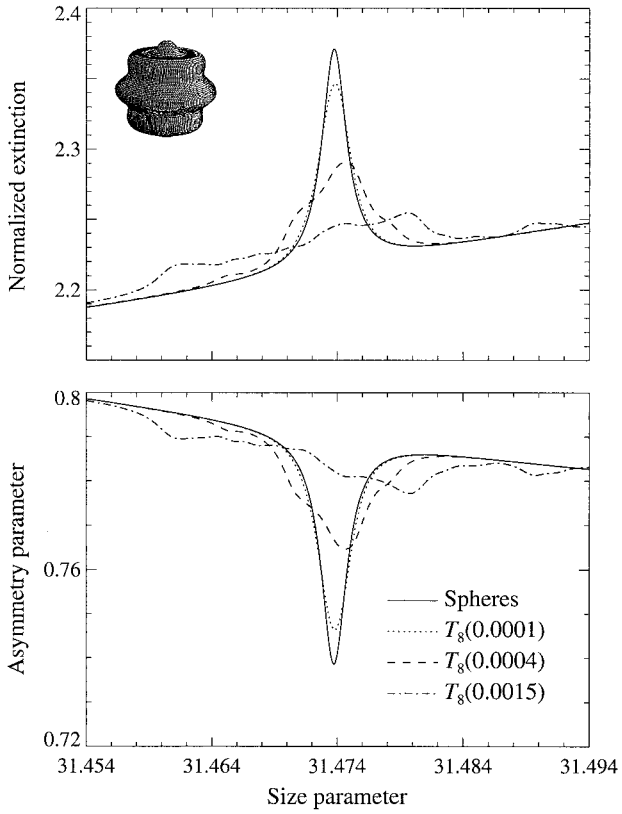

Fig. 4. As in Fig. 1, but for Chebyshev particles.

ripple is absent in the curves for the nearly spherical spheroids and is the contribution of additional natural frequencies of oscillation of distinctly aspherical spheroids with specific orientations relative to the incident beam. This effect is demonstrated in Fig. 6, which shows the normalized extinction $C_{\text{ext}}(\beta)/(\pi a^2)$ as a function of the equal-volume-sphere size parameter and the orientation angle β (the angle between the spheroid axis and the incidence direction) for prolate spheroids with $a/b = 0.9$. The incident light is assumed to be unpolarized. The overall increase of the extinction cross section C_{ext} with increasing β is explained by the growing area of the spheroid geometric projection on the plane perpendicular to the incidence direction.

3. Spheres Cut by a Plane

One trait that spheroids and Chebyshev particles have in common is that even a minute deviation of the axis ratio a/b from unity or of the deformation parameter ξ from zero distorts the entire particle surface. It would be interesting, therefore, to analyze the behavior of a SNMDR for nearly spherical particles obtained by distortion of only a small fraction of the surface of a perfect sphere. A good example of such particles are spheres cut by a plane (SCBP; Fig. 7). Such scatterers are bodies of revolution and as such can be efficiently handled by the T-matrix method. One should take into account, however, that SCBP are particles with piecewise smooth surfaces and require the application of a separate quadrature formula to each smooth part in the computation of the integrals in Eqs. (5.196)–(5.199) of Ref. 2 (compare with Refs. 9 and 10). Furthermore, the presence of a relatively sharp transition from the spherical to the plane surface of SCBP slows down the convergence rate of the T-matrix computations. Therefore we had to relax the relative computational accuracy to 10^{-5}.

It is convenient to characterize the shape of SCBP in terms of the asphericity parameter $e = (l - a)/a$, where a is the radius of the unperturbed sphere and l is the particle linear dimension along the rotation axis (Fig. 7). For example, the value $e = 1$ corresponds to a perfect sphere, whereas $e = 0$ yields a hemisphere.

Figure 8 is analogous to Figs. 1–4 but shows the results of T-matrix computations for SCBP with three increasing values of the asphericity parameter. One can see that now it takes a much larger degree of asphericity to suppress the supernarrow resonance than in the case of either spheroids or Chebyshev particles. Another striking difference is that now the position of the SNMDR remains exactly the same irrespective of the specific value of e.

4. Discussion

We hope that our findings will be taken into account and eventually reproduced by analytical and semianalytical theories intended to give a simplified quantita-

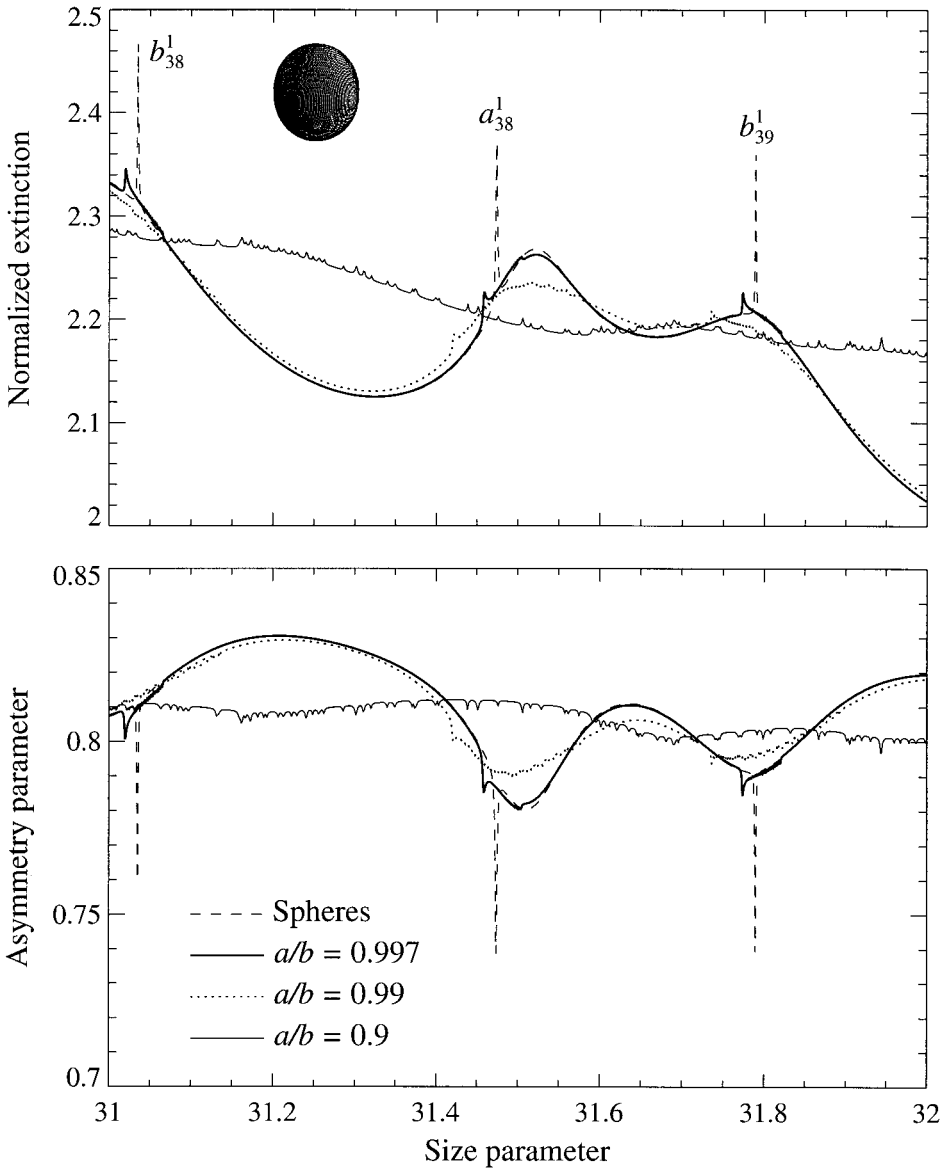

Fig. 5. As in Fig. 2, but for a wider range of size parameters. The data were computed with a size parameter step size of 0.0005.

tive description of the resonance phenomenon.[1,3,11,12] However, the fact that global surface deformations of a sphere as small as $\lambda/100$ have a profound effect on the Lorenz–Mie SNMDRs and that significantly greater surface deformations are needed to suppress the broader MDRs appears to be consistent with the traditional physical interpretation of the MDRs as that of a situation in which rays propagate around the inside surface of a sphere, confined by an almost total internal reflection.[1] After circumnavigating the sphere, the rays return to their respective entrance points exactly in phase and then follow the same path all over again without being attenuated by destructive interference. A global deformation of the sphere surface changes the phases of the rays and facilitates destructive interference, thereby suppressing the resonance. Because the width of a resonance is inversely proportional to the internal path length of the rays,[13] the SNMDRs suffer much stronger from the rapidly accumulating phase changes and are much more sensitive to increasing surface deformations than the broader MDRs. The traditional interpretation of the MDRs is also supported by our *T*-matrix results for SCBP. In this case, the spherical part of the particle surface remains significant even for rather small values of *e* and can still support the majority of the internal ray trajectories causing the SNMDR. Furthermore, the position of the resonance remains exactly the same because the radius of curvature does not change.

Another important result of this study is that it allows one to estimate the upper limit on the possible deviation of the particle shape from the perfect sphere in experiments like the one described in Ref. 14 and involving measurements of light scattering by a levitated, gradually evaporating liquid droplet. It seems obvious that nearly spherical spheroids or

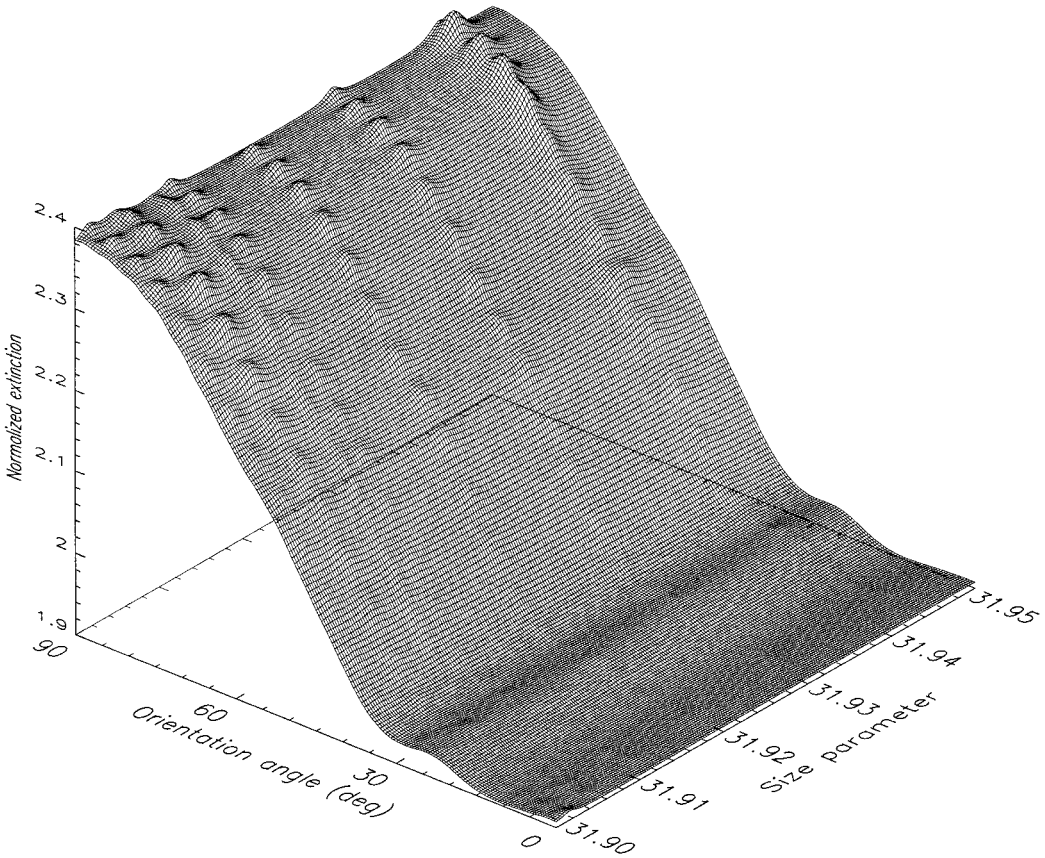

Fig. 6. Normalized extinction versus volume-equivalent-sphere size parameter and orientation angle for prolate spheroids with a relative refractive index of 1.4 and an axis ratio of $a/b = 0.9$. The data were computed with a size parameter step size of 0.00025 and an orientation angle step size of 0.5°.

Chebyshev particles afford a much more adequate model of natural deformations of a liquid droplet than SCBP. Therefore the fact that those experiments were successful in the detection of Lorenz–Mie SNMDRs implies that the scattering particles must have been extremely close to ideal spheres.

Our final comment is intended to emphasize the

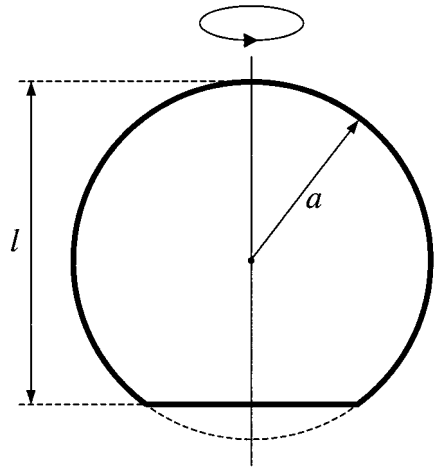

Fig. 7. Sphere cut by a plane.

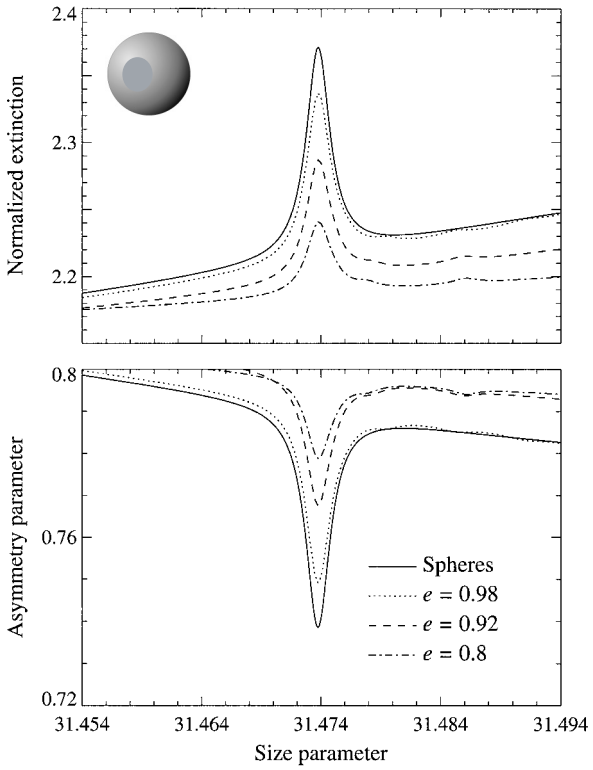

Fig. 8. As in Fig. 1, but for SCBP.

decisive importance of the *T*-matrix method for this study. Indeed, the extreme sensitivity of the SNMDRs to surface deformations as small as $\lambda/100$ makes it essentially impossible to perform a study such as this one with finite-element and volume-integral equation techniques, which traditionally use a much coarser discretization of the particle interior and surface (e.g., Refs. 15 and 16 and references therein).

We thank Nadia Zakharova for help with graphics. This research was supported by the NASA Radiation Sciences Program managed by Donald Anderson.

References

1. S. C. Hill and R. E. Benner, "Morphology-dependent resonances," in *Optical Effects Associated with Small Particles,* P. W. Barber and R. K. Chang, eds. (World Scientific, Singapore, 1988), pp. 3–61.
2. M. I. Mishchenko, L. D. Travis, and A. A. Lacis, *Scattering, Absorption, and Emission of Light by Small Particles* (Cambridge U. Press, Cambridge, UK, 2002).
3. E. J. Davis and G. Schweiger, *The Airborne Microparticle* (Springer, Berlin, 2002).
4. M. I. Mishchenko, "Light scattering by randomly oriented axially symmetric particles," J. Opt. Soc. Am. A **8,** 871–882 (1991).
5. P. C. Waterman, "Symmetry, unitarity, and geometry in electromagnetic scattering," Phys. Rev. D **3,** 825–839 (1971).
6. P. R. Conwell, P. W. Barber, and C. K. Rushforth, "Resonant spectra of dielectric spheres," J. Opt. Soc. Am. A **1,** 62–67 (1984).
7. P. Chýlek, J. T. Kiehl, and M. K. W. Ko, "Narrow resonance structure in the Mie scattering characteristics," Appl. Opt. **17,** 3019–3021 (1978).
8. W. J. Wiscombe and A. Mugnai, "Single scattering from nonspherical Chebyshev particles: a compendium of calculations," NASA Ref. Publ. NASA RP-1157 (National Aeronautics and Space Administration, Washington, D.C., 1986).
9. P. W. Barber and S. C. Hill, *Light Scattering by Particles: Computational Methods* (World Scientific, Singapore, 1990).
10. M. I. Mishchenko, L. D. Travis, and A. Macke, "Scattering of light by polydisperse, randomly oriented, finite circular cylinders," Appl. Opt. **35,** 4927–4940 (1996).
11. H. M. Nussenzveig, *Diffraction Effects in Semiclassical Scattering* (Cambridge U. Press, Cambridge, UK, 1992).
12. W. T. Grandy, *Scattering of Waves from Large Spheres* (Cambridge U. Press, Cambridge, UK, 2000).
13. G. Roll and G. Schweiger, "Geometrical optics model of Mie resonances," J. Opt. Soc. Am. A **17,** 1301–1311 (2000).
14. P. Chýlek, V. Ramaswamy, A. Ashkin, and J. M. Dziedzic, "Simultaneous determination of refractive index and size of spherical dielectric particles from light scattering data," Appl. Opt. **22,** 2302–2307 (1983).
15. M. I. Mishchenko, J. W. Hovenier, and L. D. Travis, eds., *Light Scattering by Nonspherical Particles: Theory, Measurements, and Applications* (Academic, San Diego, Calif., 2000).
16. F. M. Kahnert, "Numerical methods in electromagnetic scattering theory," J. Quant. Spectrosc. Radiat. Transfer **79/80,** 775–824 (2003).